

# T Cells Induce Extended Class II MHC Compartments in Dendritic Cells in a Toll-Like Receptor-Dependent Manner<sup>1</sup>

Marianne Boes,\* Nicolas Bertho,\* Jan Cerny,<sup>†‡§</sup> Marjolein Op den Brouw,\*  
Tomas Kirchhausen,<sup>†‡</sup> and Hidde Ploegh<sup>2\*</sup>

**Interaction of Ag-loaded dendritic cells with Ag-specific CD4 T cells induces the formation of long tubular class II MHC-positive compartments that polarize toward the T cell. We show involvement of a Toll-like receptor-mediated signal in this unusual form of intracellular class II MHC trafficking. First, wild-type dendritic cells loaded with LPS-free Ag failed to show formation of class II-positive tubules upon Ag-specific T cell engagement, but did so upon supplementation of the Ag with low concentrations of LPS. Second, Ag-loaded myeloid differentiation factor 88 -deficient dendritic cells failed to form these tubules upon interaction with T cells, regardless of the presence of LPS. Finally, inclusion of a cell-permeable peptide that blocks TNFR-associated factor 6 function, downstream of myeloid differentiation factor 88, blocked T cell-dependent tubulation. A Toll-like receptor-dependent signal is thus required to allow Ag-loaded dendritic cells to respond to T cell contact by formation of extended endosomal compartments. This activation does not result in massive translocation of class II MHC molecules to the cell surface. *The Journal of Immunology*, 2003, 171: 4081–4088.**

**T**he activation of naive T cells obligately requires the involvement of professional APCs, foremost among which are dendritic cells (DCs).<sup>3</sup> DCs express high levels of class II MHC products as well as the costimulatory molecules that render them potent activators of naive T cells. Having captured Ag at peripheral sites, DCs move to a draining lymph node where they encounter naive T cells. Somewhere between the point of Ag acquisition and the encounter with T cells in the lymph node, Ag is processed and the resulting peptides are loaded onto class II molecules. An inflammatory stimulus appears essential either for the acquisition of antigenic peptide by class II molecules or for their translocation from endosomal structures to the plasma membrane (1, 2). The display of class II-peptide complexes on the plasma membrane is required to activate CD4 T cells.

Using gene-targeted mice that express an I-A<sup>b</sup>-green fluorescent protein (GFP) fusion protein in place of I-A<sup>b</sup> molecules, we have visualized the transport of class II molecules in live bone marrow-derived DCs (3). In immature/intermediate DCs, class II MHC GFP molecules are found predominantly in internal vesicles and in short tubular compartments (~4 μm in length) which mediate constitutive delivery of class II molecules to the cell surface. Using a retroviral approach to express class II-GFP molecules, Chow et al. (4) showed that upon exposure of DCs to 0.1 μg/ml LPS, these

short tubules fuse with the plasma membrane and deliver class II molecules to the cell surface. We examined the rearrangement of class II MHC trafficking in Ag-loaded DCs confronted with Ag-specific T cells. Only when Ag-specific T cells were added to Ag-loaded DCs did we observe the rearrangement of endosomal class II-positive compartments into much longer tubular structures (average, ~20 μm in length) (3). In the current study, we focus on the priming signals in DCs to generate endosomal tubulation rather than the role of such endosomal tubules to deliver class II molecules to the cell surface. In our analyses, we quantitated numerous DC/T cell conjugates after engagement of Ag-specific T cells by analysis of still images rather than movies.

Although we used highly purified preparations of hen egg lysozyme and OVA as Ags for these initial experiments (3), the presence of low concentrations of contaminating endotoxin is likely. Even these low levels of endotoxin may deliver a signal to the DC that would then allow them to respond by tubulation toward the T cell with which it interacts. To study the effect of LPS on endosomal tubulation upon Ag-specific T cell contact, three approaches were taken. First, we extracted egg white from the sterile interior of chicken eggs as a source of LPS-free Ag. We show that LPS-free egg white fails to evoke tubulation and that addition of low concentrations of LPS restores the ability of this crude Ag preparation to induce tubule formation, but without massive translocation of class II MHC molecules to the cell surface.

Second, we generated I-A<sup>b</sup>-GFP mice deficient in the myeloid differentiation factor 88 (MyD88), an adaptor molecule recruited to the cytoplasmic tail of Toll-like receptors (TLR) 2–6 and 9 as well as IL-1 and IL-18 receptors upon their ligation (5–9). In the absence of MyD88, cells are defective in their response to LPS and CpG and, as we show here, fail to respond to Ag-specific T cells by tubulation.

Third, MyD88 may have roles in DC development as well as in their TLR-mediated activation, but to distinguish these two aspects is not always straightforward. TNFR-associated factor 6 (TRAF6) transmits signals from activated TLR and is positioned downstream of MyD88 but TRAF6 has no apparent role in DC development (10, 11). When we treated wild-type (WT)-I-A<sup>b</sup>-GFP DCs

\*Department of Pathology, <sup>†</sup>The Center for Blood Research, and <sup>‡</sup>Department of Cell Biology, Harvard Medical School, Boston, MA 02115; and <sup>§</sup>Faculty of Science, Charles University, Prague, Czech Republic

Received for publication May 12, 2003. Accepted for publication July 28, 2003.

The costs of publication of this article were defrayed in part by the payment of page charges. This article must therefore be hereby marked *advertisement* in accordance with 18 U.S.C. Section 1734 solely to indicate this fact.

<sup>1</sup> This work was supported by grants from the National Institutes of Health (to H.P. and T.K.), by a postdoctoral fellowship from the Cancer Research Institute (to M.B.), and by the Center of Molecular and Cellular Immunology (LN00A026) from the Ministry of Education, Youth and Sports of the Czech Republic (to J.C.).

<sup>2</sup> Address correspondence and reprint requests to Dr. Hidde Ploegh, Department of Pathology, Harvard Medical School, 200 Longwood Avenue, Boston, MA 02115. E-mail address: ploegh@hms.harvard.edu

<sup>3</sup> Abbreviations used in this paper: DC, dendritic cell; GFP, green fluorescent; TLR, Toll-like receptor; Myd88, myeloid differentiation factor 88; TRAF6, TNFR-associated factor 6; WT, wild type; Tf, transferrin.

with a cell permeable peptide that inhibits TRAF6 signaling (12), endosomal tubulation was impaired. Together, our data show a requirement for a microbial signal as a prerequisite for DCs to show polarized tubulation of endosomal membranes toward an interacting naive CD4 T cell.

## Materials and Methods

### Mice

I-A<sup>b</sup>-GFP knockin mice have been described previously (3). MyD88<sup>-/-</sup> mice were kindly provided by S. Akira (8). I-A<sup>b</sup>-GFP mice were crossed with MyD88<sup>-/-</sup> mice to generate I-A<sup>b</sup>-GFP-expressing mice deficient in MyD88. Genotyping for the MyD88 mutation was performed as described elsewhere (8). Mice were housed in a barrier facility and studies were performed according to institutional guidelines for animal use and care.

### Pulse-chase analysis and immunoprecipitations

Pulse-chase experiments and immunoprecipitations were performed as described previously (3, 13). Briefly, bone marrow cultures were pulsed for 45 min with 0.5  $\mu$ Ci/ml [<sup>35</sup>S]methionine/cysteine (New England Nuclear) and chased in complete DMEM for 3 h. After each chase point, cells were lysed in Nonidet P-40 lysis buffer (pH 7.4) supplemented with 1% SDS. Class II molecules were recovered by immunoprecipitation with the N22 Ab, a reagent that captures properly folded and assembled class II molecules (N22 was a gift from R. M. Steinman, Rockefeller University, New York, NY). Immunoprecipitates were recovered using Formalin-fixed staphylococcal A, washed four times with washing buffer (0.5% Nonidet P-40, 50 mM Tris-HCl (pH 7.4), 150 mM NaCl, and 5 mM EDTA), re-suspended in sample buffer containing 5% 2-ME, either boiled or kept on ice for 5 min, and analyzed by SDS-PAGE.

### Flow cytometry

DCs were characterized by expression of CD11c, with a PE-conjugated mAb to CD11c. Location of class II molecules was measured by analysis of the ratio of surface-exposed class II with a PE-conjugated mAb specific for I-A<sup>b</sup> vs I-A<sup>b</sup>-GFP, which visualizes all class II molecules irrespective of their location. Activation of DCs was measured with PE-conjugated mAb to the costimulatory molecule CD86. All fluorochrome-conjugated Abs were obtained from BD Biosciences (Mountain View, CA).

### Cell preparation and culture

DCs were generated as described previously (3, 13). In short, cells were flushed from the bone marrow cavity with PBS/2.5% FCS. Cells were plated at  $1 \times 10^6$  cells/well in 2 ml of DMEM/25 mM HEPES/10% FCS without phenol red and 10 ng/ml GM-CSF (PeproTech, Rocky Hill, NJ) and 1 ng/ml IL-4 (Roche Molecular Biochemicals, Somerville, NJ). Cells were cultured on 25-mm circular coverslips, with changes of media every second day; nonadherent cells were removed by gentle washing on days 2 and 4.

### Real-time imaging of MHC class II-GFP in bone marrow DCs

Day 5 bone marrow DCs were used for imaging. For discrimination of early and late endocytic compartments, DCs were incubated with 25  $\mu$ g/ml transferrin (Tf) Alexa Fluor 594 (early endosomes; Molecular Probes, Eugene, OR) or 25  $\mu$ g/ml lysotracker Alexa Fluor 594 (late endosomes; Molecular Probes) for 30 min at 37°C in DMEM without serum and washed three times. Images were captured with an inverted Zeiss 200M microscope equipped with a  $\times 63$  objective (1.4NA PlanApo) and a spinning wheel confocal head (PerkinElmer, Wellesley, MA). Cells were kept in a 37°C open perfusion temperature-controlled chamber (20/20 Technology, Wilmington, NC). Slidebook (Intelligent Imaging Innovation, Denver, CO) was used for image acquisition and data processing.

### Ag presentation in real time

DCs seeded at a concentration of  $1 \times 10^6$ /coverslip were incubated with 20  $\mu$ M OVA (Roche Molecular Biochemicals) or the equivalent amount of OVA in the form of crude egg white (extracted from fresh eggs; crude egg white consists for 54% of OVA (14)) for 4 h to induce display of Ag-derived peptides on class II molecules. DCs were then washed three times with media. Freshly isolated OVA-specific OTII T cells were obtained from lymph nodes from OTII-transgenic mice. T cells ( $1 \times 10^6$ ) were labeled with the nuclear dye Hoechst 33258 (Molecular Probes), washed, and added to each coverslip containing DCs. T cells were brought into contact with DCs by a 1-min centrifugation step at 1200 rpm at room temperature. Confocal microscopy analysis was done within 1 and 2 h after

T cell addition. Images were collected in a double-blind fashion and analyzed for tubulation on a separate occasion by two individuals.

### Peptides

A TRAF6-binding peptide fused with the hydrophobic sequence (AAVALL PAVLLALLAP) from Kaposi fibroblast growth factor signal sequence (L-T6DP-1) was prepared as described elsewhere (12). The TRAF6-binding decoy peptide, AAVALLPAVLLALLAP-RKIETDEYTDPRSPST, and a control peptide that has its TRAF6-binding sequence scrambled: AAVALLPAVLLALLAP-RKIEYPETDTPRSPST (signal sequence in italics and the TRAF6-binding motif and its scrambled version are underlined) were synthesized on an Advanced ChemTech 40 channel peptide synthesizer using standard F-moc chemistry. The molecular mass of each peptide was confirmed by matrix-assisted laser desorption/ionization time-of-flight mass spectrometry. DCs at a concentration of  $1 \times 10^6$ /coverslip were pretreated with decoy TRAF6 peptide or with control peptide (20  $\mu$ M, 1 h, 37°C) before following the "Ag presentation in real-time" protocol above.

### Statistical analysis

An unpaired two-tailed *t* test was used for statistical analysis. Values of *p* below 0.05 are considered significant and are given in the figure legends.

## Results

### Two-signal requirement for DCs to induce tubulation of class II MHC compartments upon addition of naive CD4 T cells

To explore the notion that DCs may need an adjuvant-like signal to allow T cell-dependent tubulation (2, 15), we prepared OVA devoid of LPS or other microbial signatures in the following manner. We extracted egg white directly from the sterile interior of fresh chicken eggs. Egg white consists of 54% (w/v) OVA (14), and this crude preparation, appropriately diluted, was used as Ag. Hereafter, crystalline OVA will be referred to as OVA and egg white extracts will be referred to as crude egg white. In contrast to commercial preparations of crystalline OVA, inclusion of crude egg white failed to activate DCs, as judged by a lack of increase in surface expression of class II MHC and CD86 after overnight culture (20  $\mu$ M normalized OVA; Fig. 1). We estimate that the batch of crystalline OVA we used contains  $\sim 1$  ng/ml LPS. By comparing T cell stimulation obtained with OVA and crude egg white to which increasing concentrations of LPS had been added, we obtained equivalent up-regulation of CD69 on naive OTII cells (TCR transgenic, I-A<sup>b</sup> restricted, OVA specific) at 1 ng/ml added LPS in crude egg white as compared with OVA (data not shown).

To visualize the intracellular distribution of class II MHC molecules, we made use of homozygous I-A<sup>b</sup>-GFP knockin mice, in which all I-A<sup>b</sup> molecules are replaced by I-A<sup>b</sup> fused at the C terminus of the  $\beta$ -chain with GFP. Such animals are phenotypically normal with respect to their immune system. We generated DCs by culture of bone marrow cells with GM-CSF and IL-4 (3). DCs are generally cultured in plastic tissue culture dishes, but for confocal

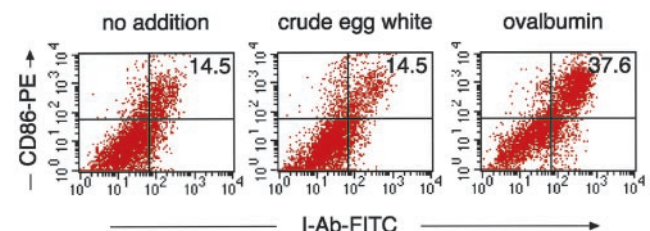


**FIGURE 1.** Activation of DCs by uptake of OVA, but not by uptake of crude egg white or in the absence of Ag. DCs were allowed to endocytose OVA and crude egg white (calculated OVA concentration for both, 20  $\mu$ M) or were left untreated and were cultured for 24 h (37°C). Activation status of DCs was analyzed the next day with flow cytometry by cell surface staining for CD86 and I-A<sup>b</sup>.

microscopy, cells must be examined on glass coverslips. We compared DCs cultured on glass coverslips with DCs maintained in plastic tissue culture dishes by staining for CD11c and CD86 and detected no significant differences in numbers or marker profiles of CD11c/class II double-positive cells. At day 5 of culture, approximately one-third of the cells expressed class II GFP, of which 80–90% expressed the DC marker CD11c and were therefore considered DCs. The majority of DCs, whether grown on plastic or glass, exhibited low levels of CD86 (data not shown).

In bone-marrow-derived DCs generated from I-A<sup>b</sup>-GFP mice and loaded with the appropriate Ag, we observed a dramatic rearrangement of endosomal compartments in response to T cells specific for that Ag (3). Tubules were classified according to their direction toward the T cell in each DC/T cell conjugate; those tubules that extend directly toward the interacting T cell are classified as “1,” tubules with a vector in the direction of, but not directly pointing at the T cell are classified as “2,” and tubules pointing away from the interacting T cell are classified as “3” (3). An example of a DC/T cell conjugate devoid of tubules, hence scored negative for categories 1, 2, and 3, is shown in Fig. 2A.

Can Ag devoid of LPS contamination induce tubulation of class II MHC compartments? We treated WT-I-A<sup>b</sup>-GFP DCs either with OVA or with crude egg white for 4 h, then washed them and exposed these DCs to naive OTII T cells. Within minutes of T cell addition, OVA-treated DCs exhibited polarized tubulation of their class II-GFP-positive compartments as reported previously (3). In contrast, in DCs exposed to crude egg white, the occurrence and length of tubulation was much reduced, yielding few projections

that were short and random in their direction. Representative conjugates are shown in Fig. 2A. When DCs were treated with crude egg white supplemented with 1 ng/ml LPS for 4 h, the extent of tubulation of endosomal class II compartments was similar to that seen in DCs treated with OVA (Fig. 2B and Table I). Increased Ag concentrations correlate with longer class II-positive tubules (3). Treatment of DCs with 1 ng/ml LPS in the absence of OVA induced only few, short class II-positive tubules. DCs therefore require a signal, likely delivered in the form of some microbial product, to allow the DCs to rearrange their endosomal apparatus in response to an Ag-specific T cell. Of note, when DCs were treated with 1 μg/ml LPS, many tubules developed, with an average length of 4 μm in random directions (data not shown; Refs. 4 and 16).

#### Normal development of bone marrow-derived DCs from MyD88-deficient mice

To examine the role of MyD88 in the activation of DCs, we compared the behavior of class II molecules in DCs from WT and MyD88<sup>-/-</sup> mice. We crossed the I-A<sup>b</sup>-GFP knockin mutation onto the MyD88<sup>-/-</sup> background and generated DCs by culture of bone marrow in the presence of IL-4 and GM-CSF from WT class II-GFP (WT-I-A<sup>b</sup>-GFP hereafter) and MyD88<sup>-/-</sup> I-A<sup>b</sup>-GFP (MyD-I-A<sup>b</sup>-GFP hereafter) mice (3, 13). For both WT and MyD88-deficient cultures, many clusters of I-A<sup>b</sup>-GFP-positive cells were present at day 5 of culture, 90% of which expressed the DC marker CD11c (Fig. 3A). As assessed by both surface staining and GFP levels, we observe a moderately reduced expression of I-A<sup>b</sup> in a subpopulation of CD11c-positive cells from the MyD-I-

**FIGURE 2.** Requirement for LPS to induce class II-positive tubules upon interaction of Ag-loaded DCs with Ag-specific T cells. *A*, DCs were left untreated or were allowed to endocytose crude egg white (20 μM OVA equivalent), LPS (1 ng/ml), and crude egg white (20 μM OVA equivalent) supplemented with LPS (1 ng/ml) or OVA (20 μM) for 4 h at 37°C, were washed twice, and naive OTII T cells, labeled with Hoechst 33258, were added. Representative images of DC/T cell conjugates of crude egg white-treated DCs (*left*) and crude egg white plus LPS-treated DCs (*right*) are shown. *B*, Tubule direction was determined relative to the interacting T cells in category 1, 2, or 3 as shown in the diagram. For each treatment of DCs, at least 39 DC/T cell conjugates were analyzed for the presence of tubulating class II-positive compartments. The percentage of tubulating DCs in the DC/T conjugates of the various treatments are shown (*left*). Of the DC/T conjugates that contain tubulating DCs, the length and direction of the tubules were measured. Shown is the mean length of the tubules in categories 1, 2, and 3 (see diagram) with SEM.

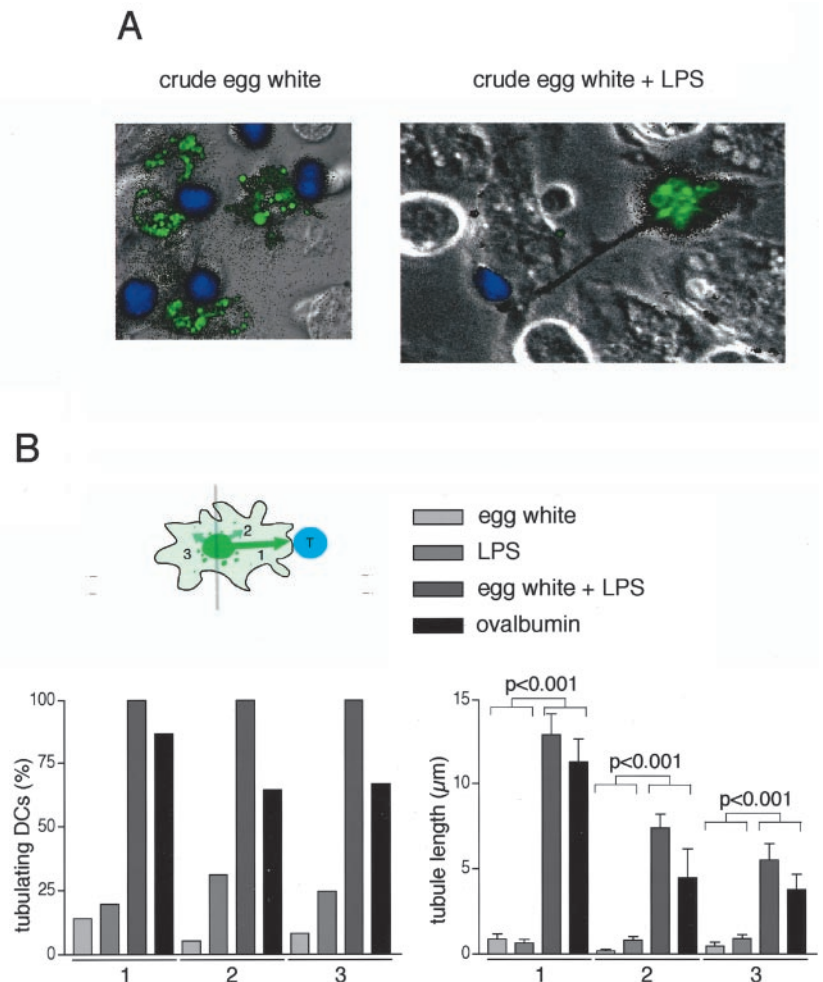


Table I. Tubule length upon Ag-specific T cell contact<sup>a</sup>

Category	Tubule Length ( $\mu\text{m}$ )			
	Egg white	LPS	Egg white/LPS	Oval
1	$6.3 \pm 0.86$ ( $n = 9$ )	$3.3 \pm 0.42$ ( $n = 12$ )	$12.9 \pm 1.3$ ( $n = 33$ )	$13.0 \pm 1.3$ ( $n = 32$ )
2	$3.4 \pm 0.40$ ( $n = 3$ )	$3.0 \pm 0.28$ ( $n = 17$ )	$7.4 \pm 0.80$ ( $n = 11$ )	$7.0 \pm 2.3$ ( $n = 9$ )
3	$5.7 \pm 1.3$ ( $n = 5$ )	$3.7 \pm 0.37$ ( $n = 15$ )	$5.5 \pm 0.96$ ( $n = 13$ )	$5.7 \pm 0.85$ ( $n = 10$ )

<sup>a</sup> Number of DC/T conjugates analyzed, respectively: 67, 61, 39, and 41.

A<sup>b</sup>-GFP DCs (Fig. 3B). Thus, the generation of DCs from bone marrow precursors in vitro is mostly normal in MyD-I-A<sup>b</sup>-GFP cells.

#### Normal endosomal localization of class II MHC molecules in MyD-I-A<sup>b</sup>-GFP DCs

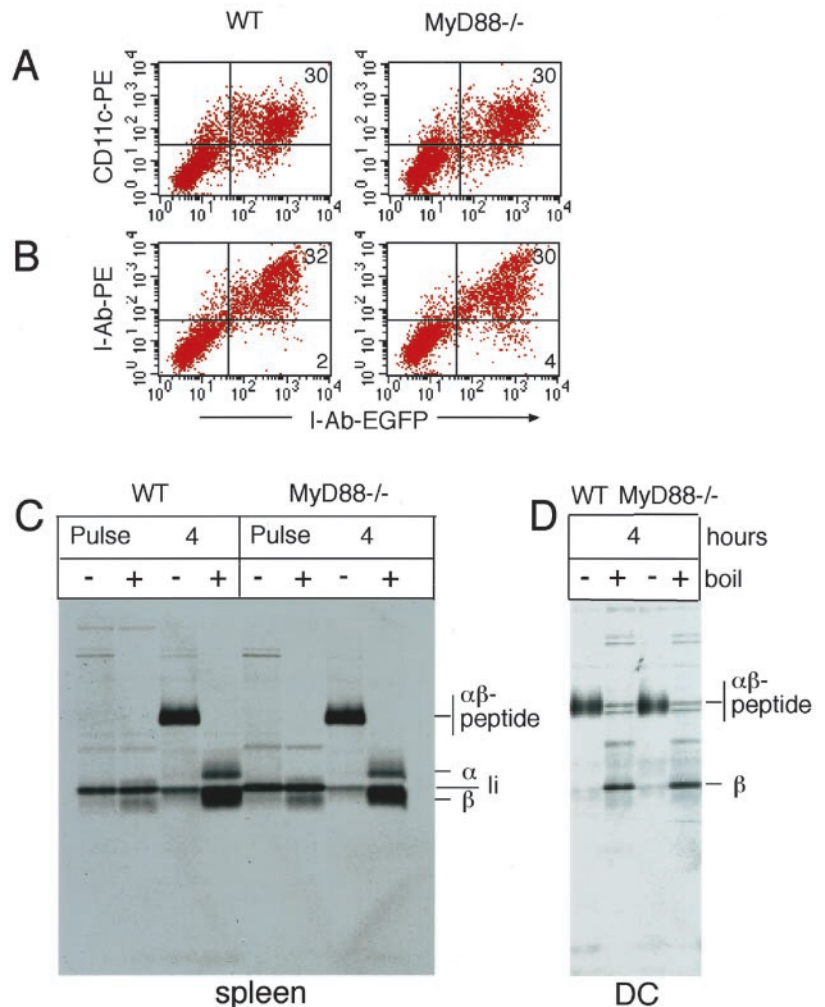
In professional APCs, at steady state, class II MHC molecules reside predominantly in endosomal compartments. Bone marrow-derived DCs were allowed to endocytose Alexa-labeled Tf, which localizes to early and recycling endosomes, and were then examined by confocal microscopy. In both WT-I-A<sup>b</sup>-GFP and MyD-I-A<sup>b</sup>-GFP DCs, little or no colocalization of class II-GFP and Tf-Alexa is seen (data not shown), consistent with the known distributions of class II MHC and the Tf receptor (3, 17–20). To determine the location of class II MHC molecules in the endosomal pathway of WT-I-A<sup>b</sup>-GFP and MyD-I-A<sup>b</sup>-GFP DCs, cells were allowed to endocytose Alexa-lysotracker (data not shown). In

GFP-positive cells, all lysotracker-labeled compartments were also class II-GFP positive, with only small quantities of class II-GFP outside of endosomal compartments. We conclude that the localization of class II MHC molecules in the MyD88<sup>-/-</sup> cells is indistinguishable from that in WT.

#### Normal peptide loading on class II molecules in MyD88-deficient DCs

Normal levels of surface expression of class II molecules at steady state do not necessarily imply that peptide loading of class II molecules occurs normally in APCs (21, 22). To exclude aberrations in biosynthesis and peptide loading of class II molecules in MyD88<sup>-/-</sup> APCs, we analyzed the rate of intracellular transport and peptide acquisition by pulse-chase analysis and examination of the SDS resistance of class II MHC molecules. Freshly isolated spleen cells and cultured bone marrow-derived DCs were obtained from WT and MyD88<sup>-/-</sup> mice. We then examined maturation and

**FIGURE 3.** Development of DCs appears to be normal in the absence of MyD88. *A* and *B*, DCs cultured from WT-I-A<sup>b</sup>-GFP and MyD-I-A<sup>b</sup>-GFP bone marrow were analyzed with flow cytometry by staining with conjugated Abs to CD11c and I-A<sup>b</sup> to show cell surface display of class II MHC. Total class II MHC was visualized by the endogenous expression of I-A<sup>b</sup>-GFP. *C* and *D*, Splenocytes (*C*) and cultured DCs (*D*) were pulse labeled for 45 min with  $0.5 \mu\text{Ci/ml}^{-1}$  [<sup>35</sup>S]methionine/cysteine and chased in complete DMEM for 4 h. Class II MHC molecules were immunoprecipitated using N22 Ab and were resuspended in sample buffer containing 5% 2-ME, either boiled or kept on ice for 5 min, and analyzed by 12.5% SDS-PAGE.



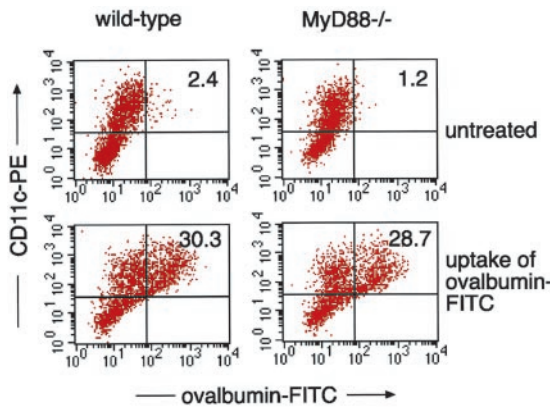


**FIGURE 4.** Normal endocytic capacity in DCs in the absence of MyD88. WT and MyD88<sup>-/-</sup> DCs were allowed to endocytose fluorescein-conjugated OVA (5 μg/ml, 30 min, 37°C). Cells were then washed and stained with conjugated Ab to CD11c and analyzed by flow cytometry. The percentage of cells in the upper right quadrant is indicated in the plots.

peptide acquisition of newly synthesized class II complexes (Fig. 3, C and D) as judged by the presence of SDS-stable dimers. Low levels of stable dimer formation were seen in freshly extracted

bone marrow and after day 3 of culture, the levels of stable class II MHC dimers increased (data not shown). At no time did we observe differences in stable dimer formation between WT and MyD88<sup>-/-</sup> APCs. Thus, the absence of MyD88 does not affect class II biosynthesis and peptide acquisition, as assessed by this method.

*Abnormal rearrangement of endosomes upon T cell engagement of MyD-I-A<sup>b</sup>-GFP DCs*

Is MyD88 required in DCs to generate tubular endosomes that polarize toward an interacting T cell? We studied the fate of class II-containing compartments in DCs upon contact with naive CD4 T cells as described previously (3). First, we determined the uptake of fluorescein-conjugated OVA by WT and MyD88<sup>-/-</sup> DCs as a measure of their endocytic capacity (Fig. 4). We obtained similar numbers of CD11c<sup>+</sup> cells from WT and MyD88<sup>-/-</sup> bone marrow cultures (Fig. 4, top panels) and found that their ability to endocytose OVA was indistinguishable (Fig. 4, bottom panels). Thus, the MyD88 deficiency does not affect endocytosis of soluble OVA in bone marrow-derived DCs.

Does MyD88 have a role in the formation of class II MHC-positive tubules induced by Ag-specific T cell ligation (3)? Bone marrow-derived DCs from WT and MyD88<sup>-/-</sup> mice were pulsed

**FIGURE 5.** Requirement for a MyD88-dependent signal to induce class II-positive tubules upon interaction of Ag-loaded DCs with Ag-specific T cells. DCs cultured from WT-I-A<sup>b</sup>-GFP and MyD-I-A<sup>b</sup>-GFP bone marrow were allowed to endocytose OVA for 4 h (20 μM, 37°C), were washed twice, and naive OTII T cells, labeled with Hoechst 33258, were added. Confocal microscopy was done between 1 and 2 h of T cell addition. Representative images of DC/T cell conjugates of WT-I-A<sup>b</sup>-GFP DCs (left) and MyD-I-A<sup>b</sup>-GFP DCs (right) are shown. B, For WT DCs, 35 DC/T conjugates with naive OTII T cells were analyzed; for MyD88<sup>-/-</sup> DCs, 57 DC/T conjugates were analyzed. The percentage of tubulating DCs in the DC/T conjugates for WT-I-A<sup>b</sup>-GFP and MyD-I-A<sup>b</sup>-GFP are shown (left). Of the DC/T conjugates that contain tubulating DCs, the length and direction of the tubules were measured. Shown is the mean length of the tubules in categories 1, 2, and 3 (see diagram) with SEM.

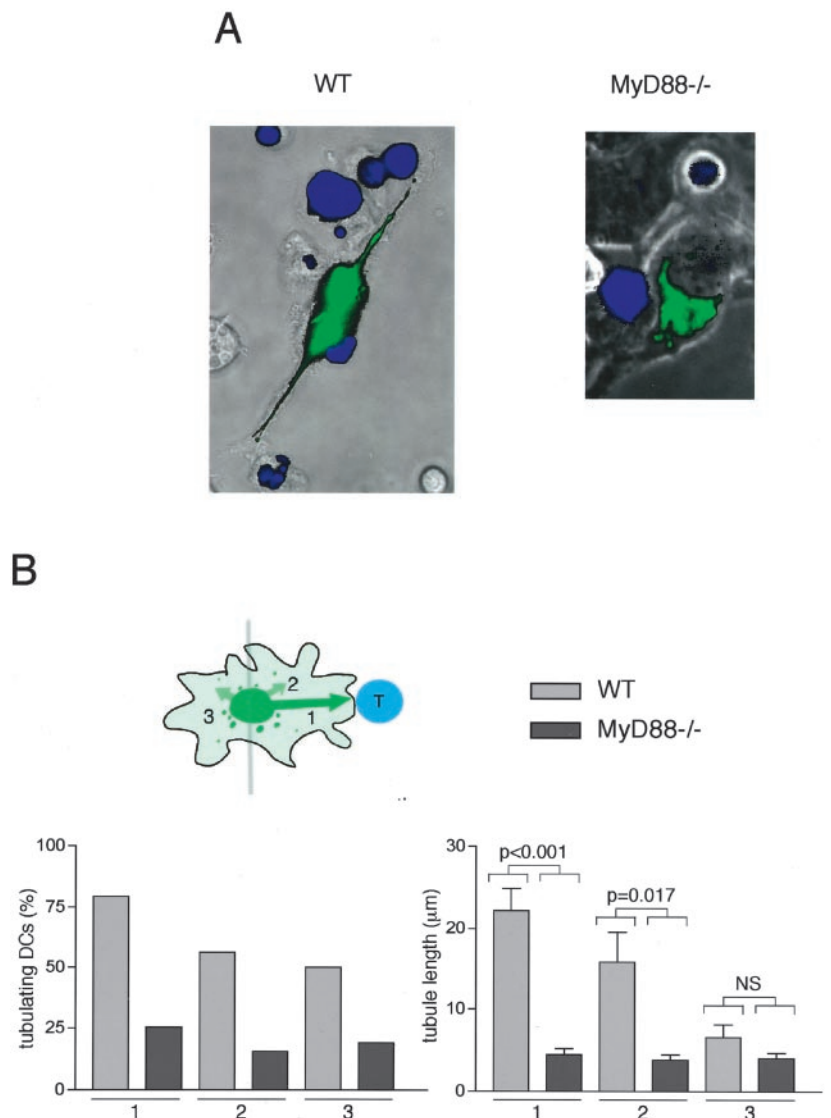


Table II. Tubule length upon Ag-specific T cell contact<sup>a</sup>

Category	Tubule Length ( $\mu\text{m}$ )	
	WT	MyD88 <sup>-/-</sup>
1	22.2 $\pm$ 2.7 (n = 22)	4.4 $\pm$ 0.78 (n = 7)
2	15.8 $\pm$ 3.8 (n = 9)	3.9 $\pm$ 0.59 (n = 7)
3	6.6 $\pm$ 1.6 (n = 7)	4.0 $\pm$ 0.65 (n = 9)

<sup>a</sup> Number of DC/T conjugates analyzed, respectively: 35 and 57.

with OVA (20  $\mu\text{M}$ ) for 4 h and excess Ag was removed by washing. Naive OTII T cells were added and randomly selected DC/T cell conjugates were analyzed immediately by time-lapse confocal microscopy. We recorded the presence, number, and orientation of these tubules relative to the interacting T cells.

For WT-I-A<sup>b</sup>-GFP DCs, tubulation was readily apparent upon contact with Ag-specific T cells. In the presented image, tubulation was bipolar, directed toward both interacting T cells (Fig. 5A, left). In contrast, in the MyD-I-A<sup>b</sup>-GFP DC/T cell conjugates, no such tubulation of class II-positive compartments occurred (Fig. 5A, right). Of 57 MyD88<sup>-/-</sup> DC/T cell conjugates analyzed, the overall average length of tubules was 4  $\mu\text{m}$ , whereas in the WT DCs, the average length of category 1, 2 and 3 tubules was 22.2, 15.8,

Table III. Tubule length upon Ag-specific T cell contact<sup>a</sup>

Category	Tubule Length ( $\mu\text{m}$ )	
	TRAF6 scrambled	TRAF6 decoy
1	13.7 $\pm$ 1.1 (n = 50)	6.6 $\pm$ 1.1 (n = 16)
2	8.6 $\pm$ 1.7 (n = 12)	4.3 $\pm$ 0.70 (n = 6)
3	4.1 $\pm$ 0.77 (n = 12)	3.7 $\pm$ 0.64 (n = 10)

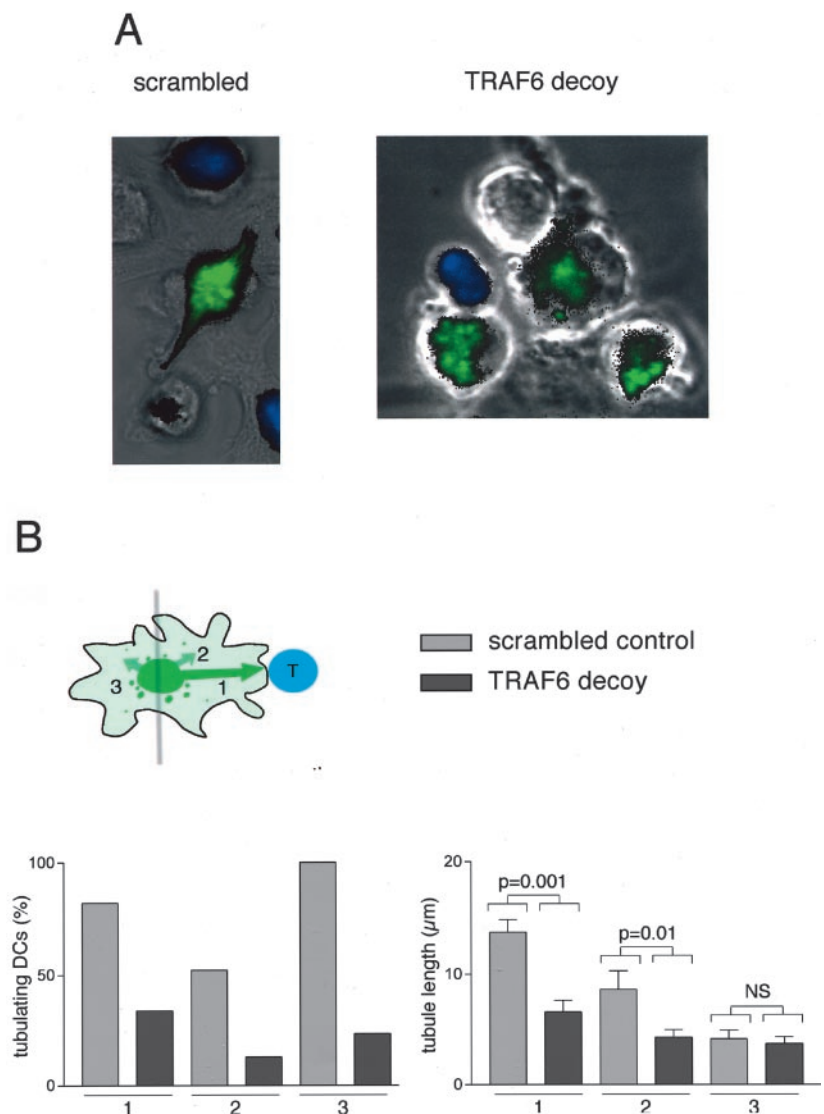
<sup>a</sup> Number of DC/T conjugates analyzed, respectively: 59 and 47.

and 6.6  $\mu\text{m}$ , respectively (Fig. 5B and Table II). The few tubulations observed in MyD88<sup>-/-</sup> DCs were of no preferred orientation and were of much reduced length, perhaps similar to the tubules observed in DCs in the absence of Ag (3, 4, 16). A quantitation of the tubule length, orientation, and frequency is given in Table II. Thus, DCs require MyD88 for rapid induction of tubular class II-positive compartments induced by Ag-specific T cell ligation.

#### TRAF6 signaling requirement for class II-positive tubule formation

Ligation of TLR with microbial products results in recruitment of MyD88 to the cytoplasmic region of a TLR. The bound MyD88 then recruits IL-1R-associated kinase to the receptor, which upon

**FIGURE 6.** Signaling through TRAF6 is required to induce class II-positive tubules upon interaction of Ag-loaded DCs with Ag-specific T cells. **A**, DCs cultured from WT-I-A<sup>b</sup>-GFP bone marrow were pre-treated with cell-permeable peptide containing either a decoy sequence for TRAF6 or a scrambled sequence (see *Materials and Methods*; 20  $\mu\text{M}$ , 1 h, 37°C) before addition of OVA for 4 h (20  $\mu\text{M}$ , 37°C). DCs were washed twice and naive OTII T cells, labeled with Hoechst 33258, were added. Confocal microscopy was done between 1 and 2 h after T cell addition. Representative images of DC/T cell conjugates of scrambled peptide-treated WT-I-A<sup>b</sup>-GFP DCs (left) and TRAF6 decoy peptide-treated WT-I-A<sup>b</sup>-GFP DCs (right) are shown. **B**, We analyzed 59 DC/T conjugates of scrambled peptide-treated DCs and 47 DC/T conjugates of TRAF6 decoy peptide-treated DCs. The percentage of tubulating DCs in the DC/T conjugates for scrambled peptide and TRAF6 decoy peptide-treated DCs are shown (left). Of the DC/T conjugates that contain tubulating DCs, the length and direction of the tubules were measured. Shown is the mean length of the tubules in categories 1, 2, and 3 (see diagram) with SEM.



activation is released from the receptor complex and binds and activates TRAF6 for stimulation of the I $\kappa$ B kinase complex, mitogen-activated protein kinase (9), and possibly other kinases as well. The phenotype of TRAF6-deficient mice shows that TRAF6 is essential for cellular responses to LPS and IL-1 (10, 23). Cell-permeable peptides that can form a complex with TRAF6 have been used successfully as decoys to inhibit TRAF6 signaling (12).

Can DCs in which TRAF6 signaling is inhibited still induce tubulation of class II MHC compartments? We synthesized a cell-permeable TRAF6 decoy and a scrambled control peptide (Fig. 6A; Ref. 12) and pretreated WT-I-A<sup>b</sup>-GFP DCs with peptide (20  $\mu$ M, 1 h at 37°C) before addition of crystalline OVA. DCs were allowed to endocytose OVA for 4 h and then washed and exposed to naive OTII T cells. In WT-I-A<sup>b</sup>-GFP cells treated with a peptide in which the TRAF6-binding sequence is scrambled, contacts between T cells and DCs result in pronounced tubulation of class II-positive compartments toward the T cell. In DC/T cell conjugates treated with the TRAF6 decoy peptide, no such tubulation of class II-positive compartments occurred (Fig. 6B). On average, the tubule length for TRAF6 decoy-treated DCs was 4.9  $\mu$ m, whereas in the experiment shown for the control peptide-treated DCs, the average lengths of category 1, 2, and 3 tubules were 13.7, 8.6, and 4.1  $\mu$ m, respectively (Fig. 6B and Table III). Thus, DCs require a priming event through TLR ligation to induce class II-positive tubular endosomes upon interaction with Ag-specific T cells, yet such activation does not entail massive translocation of class II MHC molecules to the cell surface.

## Discussion

When DCs mature, peptide-loaded class II MHC molecules are transported from endosomal compartments to the plasma membrane for display to CD4 T cells. Under inflammatory circumstances, Ag-experienced DCs activate naive CD4 T cells and a step crucial for induction of the adaptive immune response. A thorough understanding of the activation requirements of DCs that lead to translocation of class II MHC molecules to the plasma membrane in DCs is thus essential. We studied here the DC priming requirements to undergo endosomal rearrangements to form T cell polarized tubular structures.

Using bone marrow-derived DCs from I-A<sup>b</sup>-GFP knockin animals, we showed that Ag-loaded DCs interact with Ag-specific naive T cells and rearrange their class II-positive endosomal compartments into tubular structures of considerable length. This tubulation was seen in the absence of added LPS and was strictly Ag dependent. Still, LPS contamination of commercial Ags is a well-known occurrence and raises the question whether this mode of tubulation is dependent only on an Ag-specific encounter with an appropriate T cell, or whether an additional factor (e.g., a TLR-delivered signal) is required that may prime DCs for this behavior.

As a source of LPS-free Ag, we used crude egg white extracted directly from a chicken egg and compared it with OVA obtained commercially. Treatment with OVA resulted in prominent tubulation upon interaction with Ag-specific T cells, but treatment with crude egg white did not. Addition of LPS (1 ng/ml) to crude egg white restored tubulation to the same extent as that observed when treated with commercial OVA. Of note, at this concentration of added LPS, no massive translocation of class II molecules to the cell surface occurs.

The presence of LPS is detected by DCs through ligation of TLR4, which uses the adapter molecule MyD88 and TRAF6 for signal transduction to the nucleus (24). MyD88<sup>-/-</sup> DCs consistently failed to respond to an Ag-specific encounter by tubulation, even though synthesis and maturation of class II MHC molecules occur normally, and surface expression of class II MHC molecules

in immature DCs is affected only very slightly, if at all. A 1-h treatment of WT-I-A<sup>b</sup>-GFP DCs with cell-permeable inhibitory peptide to TRAF6 also prevented Ag-specific T cell ligation-induced tubulation. These results are fully consistent with those shown for the comparison between endotoxin-free Ag and the commercially available Ag preparation. We may thus consider tubulation a sign of activation of DCs, a state apparently distinct from that provoked by exposure to a high concentration of LPS in the absence of T cells or Ag.

All experiments described here involve TLR signaling as a prerequisite for the development of tubular endosomes and were analyzed for DC/T cell conjugates. Tubular class II-positive endosomes depend on the correct combination of Ag and T cell specificity (3). The majority of these tubules are T cell directed, but we observe the occurrence of occasional T cell-independent tubulation as well. Indeed, T cell-independent tubulation of endosomal compartments was described before, after treatment of the DCs at concentrations of LPS of 100 ng/ml or higher (4, 16). The tubular endosomes observed were  $\sim$ 5  $\mu$ m in length or less (4, 16). Under our experimental conditions, we established the involvement of contaminating amounts of LPS (in the order of 1 ng/ml) present in the Ag in the formation of T cell-polarized endosomal tubulation. Tubular endosomes described here may originate from the same source as the LPS-induced tubules. Their polarization toward Ag-specific T cells and their length indicates a role in the transport of peptide-loaded class II MHC molecules to the site of T cell contact.

Signaling events initiated by TLR ligation involve initiation of transcription of genes that encode costimulatory products such as CD86, CD80, and CD40 and of inflammatory cytokine genes such as TNF- $\alpha$  and IFN- $\gamma$  (25). MyD88<sup>-/-</sup> cells are unable to produce IL-12 and TNF- $\alpha$  upon ligation of TLR 2, 4, and 9 (25–27). Bone marrow-derived MyD88<sup>-/-</sup> DCs are defective in class II MHC-restricted presentation, as demonstrated by their reduced ability to activate naive CD4 T cells after exposure to heat-killed and dried *Mycobacterium tuberculosis* (24). In vitro, MyD88 is dispensable in activation of Ag-specific or allogeneic T cells by DCs in 3-day coculture experiments (28), which at first sight appears at variance with our data, that show a MyD88 requirement for the formation of tubular endosomes. After 3 days of coculture of DCs with T cells in vitro, sufficient quantities of peptide-loaded class II MHC will likely have reached the cell surface and the MyD88 requirement may no longer be critical.

LPS activates DCs in vitro via TLR4 in a manner that is mostly dependent on MyD88<sup>-/-</sup>, yet can be bypassed (26, 28, 29). This bypass requires high doses of LPS (between 0.1 and 1  $\mu$ g/ml) (4, 13), far more than the LPS concentration necessary and sufficient for tubulation. Concentrations of LPS in the 0.1–1  $\mu$ g/ml range are used to generate mature DCs from less mature precursors, a process accompanied by massive translocation of class II MHC molecules to the cell surface (4, 13). Whether such concentrations resemble those encountered in the course of an infection in vivo is not known.

Based on the results presented here, we should like to propose a two-signal model for DC activation that may not require massive translocation of class II MHC molecules to the surface of DCs. The priming of DCs occurs when low amounts of microbial signatures are present, which may be in the physiological range during the pathogenic insult. Such priming may also be sufficient to render DCs responsive to appropriate chemokine gradients and allow them to migrate to draining lymph nodes (30). After priming, the DC retains the majority of its loaded class II MHC molecules sequestered in endosomes. Only little class II MHC needs to be delivered to the cell surface to allow the initial engagement of an

Ag-specific T cell. Upon arrival of DCs in a draining lymph node, rapid transport of further class II MHC molecules to the plasma membrane may occur via sustained tubulation. DCs require a microbial priming signal to IL-12 p70 production after ligation of cell surface CD40 (31). Immature DCs express very little CD40, but display CD40 within hours of microbial stimulation. Moreover, naive Ag-specific T cells express CD40 ligand only following TCR stimulation (32). In the experiments described here, we used naive T cells and therefore the extended endosomes are unlikely to be the consequence of a CD40-CD40 ligand-mediated signaling cascade.

Having encountered an Ag-specific T cell, tubulation may be beneficial for the contacting Ag-specific T cell to experience serial triggering of its T cell receptors (33–36). Activation of a naive T cell requires prolonged interaction with an APC and presumably sustained delivery of class II molecules to the site of contact between DCs and T cells. Nonetheless, we have yet to demonstrate that class II MHC molecules contained in these long tubules are in fact delivered to the cell surface. The technical limitations of total internal reflection fluorescence microscopy restrict a direct observation of fusion events to those that occur at the interface of the cell and the coverslip on which it is grown. This limitation notwithstanding, a state of DC activation may be defined that requires the two types of signal discussed above: a microbial signature and a T cell-dependent event. Imaging of DCs in lymph node *in situ*, with circulation and lymphatic drainage intact, will be required to establish whether the behavior of DCs, as seen here *in vitro*, applies equally to DCs *in vivo*.

## Acknowledgments

We acknowledge members in the Ploegh laboratory for helpful discussions. We thank Edda Fiebiger, Eckart Schott, and Justine Mintern for critical reading of this manuscript.

## References

- Inaba, K., S. Turley, T. Iyoda, F. Yamaide, S. Shimoyama, C. Reis e Sousa, R. N. Germain, I. Mellman, and R. M. Steinman. 2000. The formation of immunogenic major histocompatibility complex class II-peptide ligands in lysosomal compartments of dendritic cells is regulated by inflammatory stimuli. *J. Exp. Med.* 191:927.
- Turley, S. J., K. Inaba, W. S. Garrett, M. Ebersold, J. Unternaehrer, R. M. Steinman, and I. Mellman. 2000. Transport of peptide-MHC class II complexes in developing dendritic cells. *Science* 288:522.
- Boes, M., J. Cerny, R. Massol, M. Op den Brouw, T. Kirchhausen, J. Chen, and H. L. Ploegh. 2002. T-cell engagement of dendritic cells rapidly rearranges MHC class II transport. *Nature* 418:983.
- Chow, A., D. Toomre, W. Garrett, and I. Mellman. 2002. Dendritic cell maturation triggers retrograde MHC class II transport from lysosomes to the plasma membrane. *Nature* 418:988.
- Wesche, H., W. J. Henzel, W. Shillinglaw, S. Li, and Z. Cao. 1997. MyD88: an adapter that recruits IRAK to the IL-1 receptor complex. *Immunity* 7:837.
- Muzio, M., J. Ni, P. Feng, and V. M. Dixit. 1997. IRAK (Pelle) family member IRAK-2 and MyD88 as proximal mediators of IL-1 signaling. *Science* 278:1612.
- Medzhitov, R., P. Preston-Hurlburt, E. Kopp, A. Stadlen, C. Chen, S. Ghosh, and C. A. Janeway, Jr. 1998. MyD88 is an adaptor protein in the hToll/IL-1 receptor family signaling pathways. *Mol. Cell* 2:253.
- Adachi, O., T. Kawai, K. Takeda, M. Matsumoto, H. Tsutsui, M. Sakagami, K. Nakanishi, and S. Akira. 1998. Targeted disruption of the MyD88 gene results in loss of IL-1- and IL-18-mediated function. *Immunity* 9:143.
- Takeuchi, O., and S. Akira. 2002. Genetic approaches to the study of Toll-like receptor function. *Microbes Infect.* 4:887.
- Naito, A., S. Azuma, S. Tanaka, T. Miyazaki, S. Takaki, K. Takatsu, K. Nakao, K. Nakamura, M. Katsuki, T. Yamamoto, and J. Inoue. 1999. Severe osteopetrosis, defective interleukin-1 signalling and lymph node organogenesis in TRAF6-deficient mice. *Genes Cells* 4:353.
- Wong, B. R., D. Besser, N. Kim, J. R. Arron, M. Vologodskaya, H. Hanafusa, and Y. Choi. 1999. TRANCE, a TNF family member, activates Akt/PKB through a signaling complex involving TRAF6 and c-Src. *Mol. Cell* 4:1041.
- Ye, H., J. R. Arron, B. Lamothe, M. Cirilli, T. Kobayashi, N. K. Shevde, D. Segal, O. K. Dzivenu, M. Vologodskaya, M. Yim, et al. 2002. Distinct molecular mechanism for initiating TRAF6 signalling. *Nature* 418:443.
- Cella, M., A. Engering, V. Pinet, J. Pieters, and A. Lanzavecchia. 1997. Inflammatory stimuli induce accumulation of MHC class II complexes on dendritic cells. *Nature* 388:782.
- Awade, A. C. 1996. On hen egg fractionation: applications of liquid chromatography to the isolation and the purification of hen egg white and egg yolk proteins. *Z. Lebensm.-Unters.-Forsch.* 202:1.
- Kleijmeer, M., G. Ramm, D. Schuurhuis, J. Griffith, M. Rescigno, P. Ricciardi-Castagnoli, A. Y. Rudensky, F. Ossendorp, C. J. Melief, W. Stoorvogel, and H. J. Geuze. 2001. Reorganization of multivesicular bodies regulates MHC class II antigen presentation by dendritic cells. *J. Cell Biol.* 155:53.
- Villadangos, J. A., M. Cardoso, R. J. Steptoe, D. van Berkel, J. Pooley, F. R. Carbone, and K. Shortman. 2001. MHC class II expression is regulated in dendritic cells independently of invariant chain degradation. *Immunity* 14:739.
- Kleijmeer, M. J., S. Morkowski, J. M. Griffith, A. Y. Rudensky, and H. J. Geuze. 1997. Major histocompatibility complex class II compartments in human and mouse B lymphoblasts represent conventional endocytic compartments. *J. Cell Biol.* 139:639.
- Nijman, H. W., M. J. Kleijmeer, M. A. Ossevoort, V. M. Oorschot, M. P. Vierboom, M. van de Keur, P. Kenemans, W. M. Kast, H. J. Geuze, and C. J. Melief. 1995. Antigen capture and major histocompatibility class II compartments of freshly isolated and cultured human blood dendritic cells. *J. Exp. Med.* 182:163.
- Peters, P. J., J. J. Neefjes, V. Oorschot, H. L. Ploegh, and H. J. Geuze. 1991. Segregation of MHC class II molecules from MHC class I molecules in the Golgi complex for transport to lysosomal compartments. *Nature* 349:669.
- Peters, P. J., G. Raposo, J. J. Neefjes, V. Oorschot, R. L. Leijendekker, H. J. Geuze, and H. L. Ploegh. 1995. Major histocompatibility complex class II compartments in human B lymphoblastoid cells are distinct from early endosomes. *J. Exp. Med.* 182:325.
- Villadangos, J. A., R. A. Bryant, J. Deussing, C. Driessen, A. M. Lennon-Dumenil, R. J. Riese, W. Roth, P. Saffig, G. P. Shi, H. A. Chapman, et al. 1999. Proteases involved in MHC class II antigen presentation. *Immunity* 10:109.
- Nakagawa, T. Y., W. H. Brissette, P. D. Lira, R. J. Griffiths, N. Petrusheva, J. Stock, J. D. McNeish, S. E. Eastman, E. D. Howard, S. R. Clarke, et al. 1999. Impaired invariant chain degradation and antigen presentation and diminished collagen-induced arthritis in cathepsin S null mice. *Immunity* 10:207.
- Lomaga, M. A., W. C. Yeh, I. Sarosi, G. S. Duncan, C. Furlonger, A. Ho, S. Morony, C. Capparelli, G. Van, S. Kaufman, et al. 1999. TRAF6 deficiency results in osteopetrosis and defective interleukin-1, CD40, and LPS signaling. *Genes Dev.* 13:1015.
- Schnare, M., G. M. Barton, A. C. Holt, K. Takeda, S. Akira, and R. Medzhitov. 2001. Toll-like receptors control activation of adaptive immune responses. *Nat. Immunol.* 2:947.
- Takeuchi, O., K. Takeda, K. Hoshino, O. Adachi, T. Ogawa, and S. Akira. 2000. Cellular responses to bacterial cell wall components are mediated through MyD88-dependent signaling cascades. *Int. Immunol.* 12:113.
- Kawai, T., O. Adachi, T. Ogawa, K. Takeda, and S. Akira. 1999. Unresponsiveness of MyD88-deficient mice to endotoxin. *Immunity* 11:115.
- Hacker, H., R. M. Vabulas, O. Takeuchi, K. Hoshino, S. Akira, and H. Wagner. 2000. Immune cell activation by bacterial CpG-DNA through myeloid differentiation marker 88 and tumor necrosis factor receptor-associated factor (TRAF) 6. *J. Exp. Med.* 192:595.
- Kaisho, T., O. Takeuchi, T. Kawai, K. Hoshino, and S. Akira. 2001. Endotoxin-induced maturation of MyD88-deficient dendritic cells. *J. Immunol.* 166:5688.
- Hong, T., G. M. Barton, and R. Medzhitov. 2001. TRAP: an adapter molecule in the Toll signaling pathway. *Nat. Immunol.* 2:835.
- Randolph, G. J. 2001. Dendritic cell migration to lymph nodes: cytokines, chemokines, and lipid mediators. *Semin. Immunol.* 13:267.
- Schulz, O., A. D. Edwards, M. Schito, J. Aliberti, S. Manickasingham, A. Sher, and C. Reis e Sousa. 2000. CD40 triggering of heterodimeric IL-12 p70 production by dendritic cells *in vivo* requires a microbial priming signal. *Immunity* 13:453.
- Ise, W., M. Totsuka, Y. Sogawa, A. Ametani, S. Hachimura, T. Sato, Y. Kumagai, S. Habu, and S. Kaminogawa. 2002. Naive CD4+ T cells exhibit distinct expression patterns of cytokines and cell surface molecules on their primary responses to varying doses of antigen. *J. Immunol.* 168:3242.
- Valitutti, S., S. Muller, M. Cella, E. Padovan, and A. Lanzavecchia. 1995. Serial triggering of many T-cell receptors by a few peptide-MHC complexes. *Nature* 375:148.
- Underhill, D. M., M. Bassetti, A. Rudensky, and A. Aderem. 1999. Dynamic interactions of macrophages with T cells during antigen presentation. *J. Exp. Med.* 190:1909.
- Gunzer, M., A. Schafer, S. Borgmann, S. Grabbe, K. S. Zanker, E. B. Brocker, E. Kampgen, and P. Friedl. 2000. Antigen presentation in extracellular matrix: interactions of T cells with dendritic cells are dynamic, short lived, and sequential. *Immunity* 13:323.
- Irvine, D. J., M. A. Purbhoo, M. Krosgaard, and M. M. Davis. 2002. Direct observation of ligand recognition by T cells. *Nature* 419:845.